Low-pass spatial filtering using a two-dimensional self-collimating photonic crystal

Zhixiang Tang (唐志祥)[1,2], Dianyuan Fan (范滇元)[2], Shuangchun Wen (文双春)[1], Yunxia Ye (叶云霞)[2], and Chujun Zhao (赵楚军)[2]

[1]*School of Computer and Communication, Hu'nan University, Changsha 410082*

[2]*Shanghai Institute of Optics and Fine Mechanics, Chinese Academy of Sciences, Shanghai 201800*

Different from previous focusing on subwavelength imaging in the near field, we outline another potentially useful application of the self-collimating photonic crystal — low-pass spatial filtering. A two-dimensional square-lattice photonic crystal is taken as an example and the low-pass spatial filtering is demonstrated by the dispersion analysis and numerical simulations. The high-spatial-frequency components, whose incident angles exceed a critical value, are reflected totally because no Bloch modes of the photonic crystal can be excited. However, the low-spatial-frequency components are coupled to the self-collimating modes and permeate the photonic crystal with high transmissivity.

OCIS codes: 330.6110, 230.0230.

A photonic crystal (PC) is an artificial medium whose refractive index is periodically arranged[1,2]. When propagating in the PCs, electromagnetic waves will be modulated in the form of Bloch modes and photonic band structure appears. With appropriate design, the propagation of electromagnetic wave can be controlled. For example, superprism and self-collimation have been demonstrated in PCs experimentally[3,4]. Recently, a great deal of attention has been focused on the anomalous phenomena such as negative refraction and flat slab focusing using PCs because of the experimental progresses[5−14].

In general, there are two underlying mechanisms for negative refraction in PCs[11−13]. One is left-handed behavior as being theoretically analyzed by Veselago[5]. In this case, because of simultaneous negative permittivity and permeability, in the PCs, the electromagnetic fields **E**, **H** and the wave vector **k** form a left-handed triplet (i.e. $\mathbf{S}\cdot\mathbf{k}<0$, where **S** is the Poynting vector). The other is realized without employing negative index or left-handed behavior, but by the high-order Bragg scattering[15] or anisotropy[11]. In the latter case, the PC behaves much like a right-handed medium (i.e. $\mathbf{S}\cdot\mathbf{k}>0$). This kind of negative refraction and its resulting focusing were first theoretically investigated in the partial bandgap of a two-dimensional (2D) square-lattice PC in 2002[11], and were experimentally confirmed one year after[7,10]. Subsequently, such anomalous phenomena, also called tunneling, self-guiding or self-collimating effects, have attracted a lot of attention in such PC arrays[16−18]. Here, we outline another potentially useful application of this medium — thin-film low-pass spatial filtering[19].

Low-pass spatial filters have seen many applications in the broad categories of image processing in several regions of the electromagnetic spectrum, particularly in optical spectrum. Especially in the utilization of high-power lasers, low-pass spatial filters play a very important role for beam smoothing. In the simple, traditional spatial filtering arrangement, a lens is used for focusing all spatial-frequency components, and low-, high-pass and band pass filters are implemented at the Fourier plane. The setup is, typically, at least four focal lengths long. Currently, modern spatial-frequency filtering is performed by use of interference patterns[20], anisotropic media[21], liquid-crystal cell[22], or resonator grating systems[23].

Due to controllable dispersion characteristics, we propose a simple low-pass spatial filter made from a PC that is made of dielectric rods arranged in a square lattice. In a frequency region, self-collimating phenomena can be present. With proper design, the high-spatial-frequency components, which are incident to the filter with angles exceeding a critical value, are reflected totally because no Bloch waves of the PC can be excited. However, the low-spatial-frequency components are coupled to the self-collimating modes and permeate with high transmissivity. Furthermore, this kind of filter is inherently compact. In many cases the device that is only a few wavelength thick can consist of several layers of dielectric rods.

The 2D PC used to construct a low-pass spatial filter in this paper is made of dielectric rods arranged in a square lattice. The rod has a dielectric constant of $\varepsilon = 9.2$ and a radius of $r = 1.5a$, where a is the lattice constant. For this structure, we only consider the transverse magnetic (TM) polarization, i.e., the electric field E_z is parallel to these rods. Using the plane-wave expansion method, the photonic band structure and several equifrequency contours (EFCs) are calculated and plotted in Figs. 1(a)

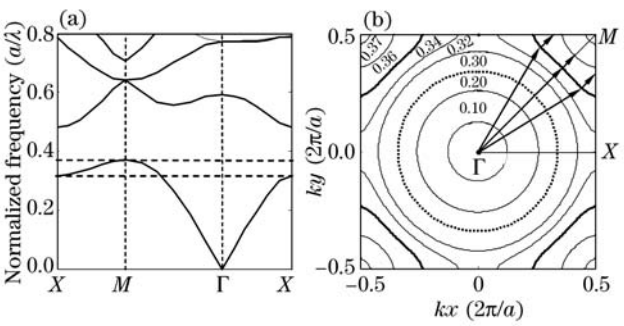

Fig. 1. Dispersion analysis of the square lattice photonic crystal.

and (b). The frequency is normalized as a/λ. According to Notomi's theory, from Figs. 1(a) and (b) we can see it clearly that in the first band the PC behaves in a right-handed manner, i.e. $\mathbf{S} \cdot \mathbf{k} > 0$[6].

In the partial bandgap (normalized frequency from 0.317 to 0.371), as shown in Fig. 1(b) EFCs within the first Brillouin zone (BZ) are significantly distorted from a circle, indicating strong anisotropy. In this case, the Bloch group velocities normalized to the EFCs are no longer collinear with their corresponding phase velocities. With the interface along TM direction, under certain conditions negative refraction occurs for the Bloch wave at the edge of the first BZ being excited[24]. Here we focus on low-pass spatial filtering using the self-collimating effect.

Take the normalized frequency $\omega = 0.34$ as an example. Due to the flat EFC shown in Fig. 1(b), strong self-collimating effect occurs at this frequency. With the interface along TM direction, the phase-matching conditions between the PC and free space are schematically analyzed in Fig. 2. It is obvious that the EFC of the free space denoted by the dotted circle is larger than that of the PC. So, the high-spatial-frequency components whose incident angles exceed the critical one β are reflected totally by the PC because no Bloch modes can be excited. However, the low-spatial-frequency components are coupled to the self-collimating modes and transmit almost perpendicularly. For this PC structure, the critical angle β equals 32°.

In order to test the above analysis, numerical simulations are conducted by using the multiple scattering method[25−27]. A 7-layer (about 1.44λ thick) PC slab is taken as an example. Two typical incident angles are performed to demonstrate the angle-dependent

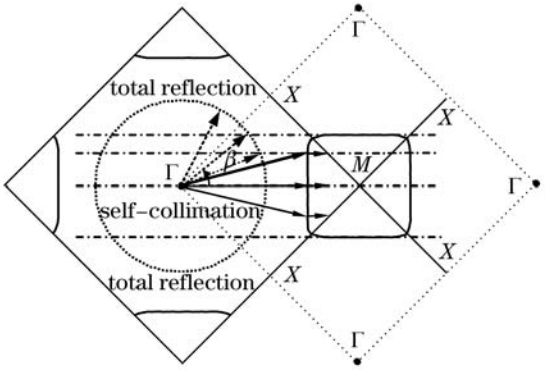

Fig. 2. Phase-matching analysis between the PC and free space.

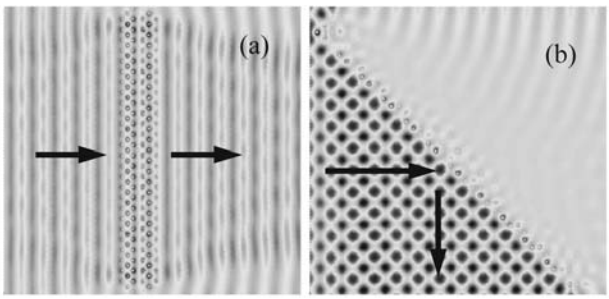

Fig. 3. Propagation maps for a plane wave incident to the PC slab with two typical angles: (a) $\alpha_1 = 0°$ and (b) $\alpha_2 = 45°$.

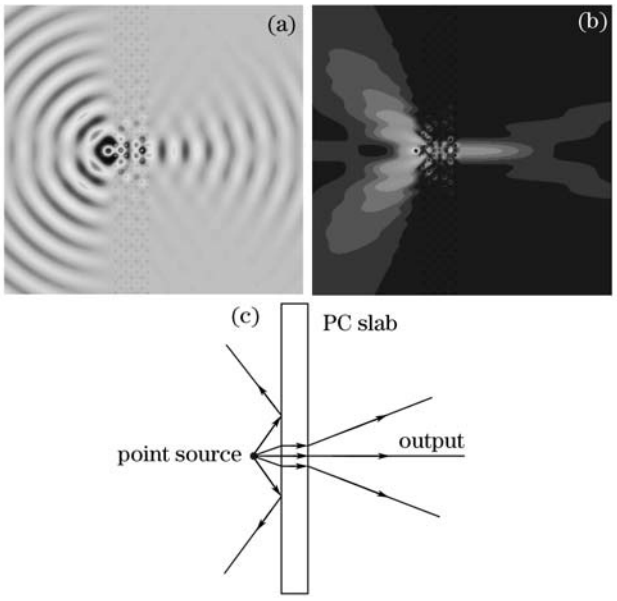

Fig. 4. Low-pass spatial filtering for a point source located at $d_0 = a$. (a) Electric-field distribution, (b) intensity distribution, (c) conceptual layout.

transmission. First, we consider a plane wave incident to the PC perpendicularly, i.e. the incident angel $\alpha_1 = 0°$. In Fig. 3(a), the incident plane wave transmits through the PC slab almost without attenuation. Because the incident angle ($\alpha_2 = 45°$) exceeds the critical one, the incident-plane waves are reflected totally as shown in Fig. 3(b). The distorted field distributions near the slab edges in Fig. 3 can be interpreted with the edge diffraction.

Due to its ability to achieve subwavelength imaging in the near field, self-collimating PCs have attracted a great deal of attention. To overcome the traditional diffraction limit, all spatial components of the source should be coupled to the self-collimating modes. However, for the PC we considered here, only the low-frequency-spatial components are canalized through the PC slab as shown in Fig. 4. Because of the total reflection of the high-frequency-spatial components, for a point source located at $d_0 = a$ before the center of the first role an image is formed near the slab with the full width at half maximum (FWHM) equaling to 0.75λ.

In conclusion, we have outlined a potentially useful application of the self-collimating PCs, low-pass spatial filtering. We have taken a square-lattice PC as an example to investigate this application simply. Dispersion characteristic analysis and numerical simulations have demonstrated that the PC is capable of low-pass spatial filtering with proper design. Due to no Bloch modes being excited, the high-spatial-frequency components whose incident angles exceeding the critical value are reflected totally by the PC. However, the low-spatial-frequency components are coupled to the self-collimating modes and transmit almost without attenuation.

This work was partially supported by the National Natural Science Foundation of China (No. 10576012 and 60538010), the National High-Technology Research and Development Program of China (No. 2004AA84ts12), and the Specialized Research Fund for the Doctoral Program of Higher Education of China (No. 20040532005).

Z. Tang's e-mail address is tangzx1000@163.com.

References

1. E. Yablonovitch, Phys. Rev. Lett. **58,** 2059 (1987).
2. S. John, Phys. Rev. Lett. **58,** 2486 (1987).
3. H. Kosaka, T. Kawashima, A. Tomita, M. Notomi, T. Tamamura, T. Sato, and S. Kawakami, Phys. Rev. B **58,** 10096 (1998).
4. H. Kosaka, T. Kawashima, A. Tomita, M. Notomi, T. Tamamura, T. Sato, and S. Kawakami, Appl. Phys. Lett. **74,** 1212 (1999).
5. V. G. Veselago, Sov. Phys. Usp. **10,** 509 (1968).
6. M. Notomi, Phys. Rev. B **62,** 10696 (2000).
7. E. Cubukcu, K. Aydin, E. Ozbay, S. Foteinopoulou, and C. M. Soukoulis, Nature **423,** 604 (2003).
8. P. V. Parimi, W. T. Lu, P. Vodo, and S. Sridhar, Nature **426,** 404 (2003).
9. Z. Tang, H. Zhang, R. Peng, Y. Ye, L. Shen, S. Wen, and D. Fan, Phys. Rev. B **73,** 235103 (2006).
10. E. Cubukcu, K. Aydin, E. Ozbay, S. Foteinopolou, and C. M. Soukoulis, Phys. Rev. Lett. **91,** 207401 (2003).
11. C. Luo, S. G. Johnson, J. D. Joannopoulos, and J. B. Pendry, Phys. Rev. B **65,** 201104 (2002).
12. Z. Tang, R. Peng, D. Fan, S. Wen, H. Zhang, and L. Qian, Opt. Express **13,** 9796 (2005).
13. R. Gajič, R. Meisels, F. Kuchar, and K. Hingerl, Opt. Express **13,** 8596 (2005).
14. R. Moussa, S. Foteinopoulou, L. Zhang, G. Tuttle, K. Guven, E. Ozbay, and C. M. Soukoulis, Phys. Rev. B **71,** 085106 (2005).
15. S. Foteinopoulou and C. M. Soukoulis, Phys. Rev. B **67,** 235107 (2003).
16. C.-H. Kuo and Z. Ye, Phys. Rev. E **70,** 026608 (2004).
17. H.-T. Chien, H.-T. Tang, C.-H. Kuo, C.-C. Chen, and Z. Ye, Phys. Rev. B **70,** 113101 (2004).
18. L.-S. Chen, C.-H. Kuo, and Z. Ye, Phys. Rev. E **69,** 066612 (2004).
19. I. Moreno, J. J. Araiza, and M. Avendano-Alejo, Opt. Lett. **30,** 914 (2005).
20. L. Dettwiller and P. Chavel, J. Opt. Soc. Am. A **1,** 18 (1984).
21. D. Schurig and D. R. Smith, Appl. Phys. Lett. **82,** 2215 (2003).
22. J.-I. Kato, I. Yamaguchi, and H. Tanaka, Opt. Lett. **21,** 767 (1996).
23. R. Rabady and I. Avrutsky, Opt. Lett. **29,** 605 (2004).
24. Z. Tang, R. Peng, Y. Ye, C. Zhao, D. Fan, H. Zhang, and S. Wen, J. Opt. Soc. Am. A **24,** 379 (2007).
25. V. Twersky, J. Acoust. Soc. Am. **24,** 42 (1951).
26. V. Twersky, J. Math. Phys. **3,** 700 (1962).
27. L.-M. Li and Z.-Q. Zhang, Phys. Rev. B **58,** 9587 (1998).